Progress in Physical Geography OnlineFirst, published on October 14, 2009 as doi:10.1177/0309133309350121

Progress in Physical Geography (2009) pp. 1–22

Problems in remote sensing of landscapes and habitats

Kai Wang,[1]* Steven E. Franklin,[1] Xulin Guo,[1] Yuhong He[2] and Gregory J. McDermid[3]

[1]Department of Geography and Planning, University of Saskatchewan, Saskatoon, SK S7N 5C8, Canada
[2]Department of Geography, University of Toronto, Mississauga, ON L5L 1C6, Canada
[3]Department of Geography, University of Calgary, Calgary, AB T2N 1N4, Canada

Abstract: Wildlife habitat mapping strongly supports applications in natural resource management, environmental conservation, impacts of anthropogenic activity, perturbed ecosystem restoration, species-at-risk recovery and species inventory. Remote sensing has long been identified as a feasible and effective technology for large-area habitat mapping. However, existing and future uncertainties in remote sensing will definitely have a significant effect on the relevant scientific research. This article attempts to identify the current challenges and opportunities in remote sensing for large-area wildlife habitat mapping, and accordingly provide possible solutions and directions for further research.

Key words: clouds and cloud shadows, data fusion, landscape pattern analysis, large-area habitat mapping, remote sensing, sensors.

I Introduction

Wildlife habitat, representing the physical space within which an organism lives, and the applicable resources (including biotic and abiotic entities; Hall *et al.*, 1997), are recognized as critical to the size of a wildlife population, playing a central role in basic and applied ecology (Mitchell, 2005). Mapping and monitoring wildlife habitat has become the key component used to interpret organism distribution, evaluate population dynamics, and predict abundance/biomass of organisms. It also strongly supports applications in natural resource management, environmental conservation, impacts of anthropogenic activity, perturbed ecosystem restoration, species-at-risk recovery, and species inventory (Mitchell, 2005;

*Author for correspondence. Email: kaw809@mail.usask.ca

DOI: 10.1177/0309133309350121

Morrison *et al.*, 2006). Most studies use physical environment characteristics when describing wildlife-habitat relationships or mapping wildlife habitat, for example land cover (Hansen *et al.*, 2001; Collingwood, 2008; McDermid *et al.*, 2008), canopy closure (Hyde, 2005), leaf area index (LAI; Chen and Black, 1992; Qi *et al.*, 2000; Li *et al.*, 2008), and so on.

Jensen (2007: 4) suggested that 'Remote sensing is the noncontact recording of information from the ultraviolet, visible, infrared, and microwave regions of the electromagnetic spectrum by means of instruments such as cameras, scanners, lasers, linear arrays, and/or area arrays located on platforms such as aircraft or spacecraft, and the analysis of acquired information by means of visual and digital image processing'. Remote sensing has long been identified as a feasible and effective technology for large-area habitat mapping (Osborne *et al.*, 2001; McDermid, 2005; Hyde, 2005), compared with *in situ* observation which has obvious limitations in time, cost and labour. However, both present and future uncertainties in remote sensing (RS) will definitely have a significant effect on scientific research regarding large-area habitats, such as the limitation of Landsat-series data, the negative impact of clouds and cloud shadows (CCS) in optical imagery, and landscape pattern analysis using RS classification products. This review focuses on three aspects relating to present and anticipated sources of uncertainty: (1) current challenges and opportunities in remote sensing; (2) possible sensors and methods to deal with these challenges and opportunities; and (3) the application issue – landscape analysis and remote sensing.

II Current challenges and opportunities in remote sensing

With the increasing abundance of RS products and RS techniques, more and more challenges and opportunities emerge. Here, we focus on three significant aspects of current challenges and opportunities: (1) the Landsat-series data in large-area habit mapping; (2) clouds and cloud shadows; and (3) data fusion.

1 The Landsat-series data in large-area habit mapping

The first satellite of the Landsat series was launched in 1972, and until 2008 the Landsat programme has provided a continued record of earth observation data for 36 years (Landsat 5 and 7 sensors are also available for delivering data). The archived images from the programme present the longest continual remotely sensed data sets available for monitoring spaced-based environment (Draeger *et al.*, 1997). Cohen and Goward (2004) have indicated that, of all remotely sensed data, data acquired by Landsat sensors have played the most pivotal role in modelling biogeochemical cycles, and also for characterizing land cover, vegetation biophysical attributes, forest structure, and fragmentation in relation to biodiversity. Franklin and Wulder (2002) argued that Landsat, due to the distinctive combination of spatial and spectral resolutions, is the best satellite sensor supporting management, monitoring, and scientific activities over large areas. In the world-famous citation database – Web of Science – users can access 5675 articles on remote sensing subject areas if the search topic is set to remote sensing. Of these, there are 2857 articles referring to Landsat, which exceeds 50% of the total (search on 20 November 2008). Wulder *et al.* (2008) concluded that the reasons for the prevalence of Landsat series are: (1) the sensor characteristics adapt perfectly to ecological application over large areas with large amounts of detail, such as the combination of spatial, spectral, and temporal resolutions, and reasonable image size; (2) a 36-year record of Landsat data makes long-term change detection commonplace; and (3) the Landsat data policy, covering data acquisition, processing, archiving, distribution, and pricing, facilitates the widespread use of data.

However, some of the Landsat characteristics restrict its application in large-area habitat mapping, including a 16-day temporal resolution, 180 km image size, and the gap of Landsat continuity. More specifically, the 16-day Landsat revisit cycle has limited Landsat's use for monitoring biodynamics (Ranson *et al.*, 2003; Roy *et al.*, 2008), and blocked the application for detecting rapid surface changes such as crop-growth monitoring and detecting intraseasonal ecosystem disturbance (Gao *et al.*, 2006; Pape and Franklin, 2008). The 185 × 185 km image size is not always suitable for the large-area applications. For example, the Foothills Research Institute Grizzly Bear Program (FRIGBP, formerly called Foothills Model Forest Grizzly Bear Research Program), initiated in 1999, is using Landsat-based products to study the relationships between landscape conditions, landscape change (human-caused), and health in grizzly bears in Alberta, Canada (Stenhouse, 2008). But the total study area should cover 273,071 km^2 (Kansas, 2002), and the 185 × 185 km size is not big enough to cover the area in a study period. Therefore, the researchers developed mosaic methods (McDermid *et al.*, 2008) to combine land-cover maps from different years forming a large map of the whole study area (ie, first divide the whole study area into several subunits; then classify a subunit per year; finally combine all of the subunits together). This classified map as a whole, cannot, however, present the updated situation of land cover, because the map of the first subunit was generated in 1999, and that of the last one in 2007 (McDermid *et al.*, 2008). It is a major problem for subsequent users, such as resource managers and ecologists.

In addition, after mapping the Earth's surface for over 30 years to meet a wide range of information needs (Chander, 2007), a gap in Landsat continuity appears unavoidable before the Landsat Data Continuity Mission data is potentially available in approximately December 2012 (as revealed by the National Aeronautics and Space Administration, NASA). The Landsat 5 TM (Thematic Mapper) sensor has been in orbit for more than 24 years, far exceeding its design life of four years, and continues to provide quality data products. Its duty cycle has been reduced and could systematically fail at any time because of the instruments' age (Chander, 2007) – note problems with the solar array drive mechanism in 2005 (Wulder *et al.*, 2008). The Landsat 7 ETM+ (Enhanced Thematic Mapper Plus) sensor failed the Scan Line Corrector (SLC) in 2003, and should have retired in 2004 (Chander, 2007). It is likely that both satellites will run out of fuel before the end of 2010 (Chander, 2007).

2 Clouds and cloud shadows

Remote sensing demonstrates a high quality of performance in many applications on account of global and repetitive measurement capability, such as scene analysis, land-use classification, landscape ecological change detection, terrain modelling, etc. However, regardless of the variety of uses for remote sensing images, the first goal is to extract landscape information from the satellite images (Tseng *et al.*, 2008). Unfortunately, two-thirds of the Earth's surface is always covered by clouds throughout the year (Wang *et al.*, 1999), causing serious problems in optical wavelength remote sensing (Wang *et al.*, 1999). Esche *et al.* (2002) also stated that since approximately 50% of the earth is covered in cloud at any given time, one of the most significant challenges in creating repeatable and robust classifications is understanding and appropriately addressing cloud contamination. Since clouds and the shadows they cast blur the optical imagery, many of the applications are impeded. For example, cloud shadow affects the accuracy of vegetation estimates, and cloud cover affects the climate system over a broad range of time and space scales (Simpson and Stitt, 1998). Asner (2001) studied cloud cover in Landsat

observations of the Brazilian Amazon and identified that clouds are a major obstacle to optical remote sensing of humid tropical regions.

Many researchers have attempted to detect clouds and the corresponding cloud shadows so as to eliminate cloud contamination producing cloud-free imagery, such as Tseng *et al.* (2008), Chen (2001), and Wang *et al.* (1999). However, numerous obstacles still exist. For example, Chen (2001) stated that the thin cloud and cloud shadow pixels had similar reflectance ranges to the cloud-free pixels; in particular, both cloud shadow and water pixels had a very similar reflectance range, and Griffin *et al.* (2003) indicated that bright surface features such as snow, ice, and sand can easily be mistaken for cloud features in the visible portion of the spectrum. Even though the locations of clouds can be detected, it is still difficult to estimate the locations of their corresponding shadows (Wang *et al.*, 1999). This is because, in some cases, the clouds and their shadows are likely to be separated by a considerable distance. The locations of shadows in the image depend on the distances of the corresponding clouds from the ground and the incidence angle of the sunlight at that time (Wang *et al.*, 1999). In addition, Esche *et al.* (2002) pointed out that the location of clouds in the scene may have an impact on the classification algorithm.

3 Data fusion

Earth observation satellites provide data that covers different portions of the electromagnetic spectrum at different spatial, temporal, and spectral resolutions. For the full exploitation of increasingly sophisticated multisource data, data fusion emerged as a new topic in the late 1980s (Gamba and Chanussot, 2008). Fused images may provide more information since data with different characteristics are combined, and consequently more reliable results obtained. A good example is the fusion of images acquired by optical sensors with data from radar sensors. Optical images reflect the spectral information of the target illuminated by sunlight, and radar intensities are sensitive to the target roughness (texture) and vertical characteristics. The fusion of these disparate data contributes to the understanding of the objects observed (Pohl and van Genderen, 1998).

a Definition of data fusion: A general definition of remotely sensed data (image) fusion is given as 'the combination of two or more different images to form a new image by using a certain algorithm' (Pohl and van Genderen, 1998: 825). Data fusion can be categorized into three groups according to the processing level where the fusion takes place: pixel, feature, and interpretation level (Figure 1). Pixel level fusion refers to the merging of measured physical parameters at the lowest processing level. It requires raster data that are at least co-registered and geocoded. Fusion at the feature level is performed after the extraction of objects recognized in the various data sources. The recognized object is called a feature, which correspond to characteristics extracted from raw images. Interpretation level fusion uses value-added data to reinforce common interpretation and furnish a better understanding of the observed data. In this level, input images are processed individually for information extraction.

Apart from the processing levels, data fusion can be applied to various types of data sets:

- single sensor for temporal, eg, multitemporal analysis of ERS-1 (European Remote Sensing satellite) SAR (Synthetic Aperture Radar) images over land areas (Weydahl, 1993);
- multisensor for temporal, eg, VIR/SAR image fusion (Pohl and van Genderen, 1995);
- single sensor for spatial, eg, pansharpening, ie, high/low resolution panchromatic/multispectral images (Ranchin and Wald, 2000);

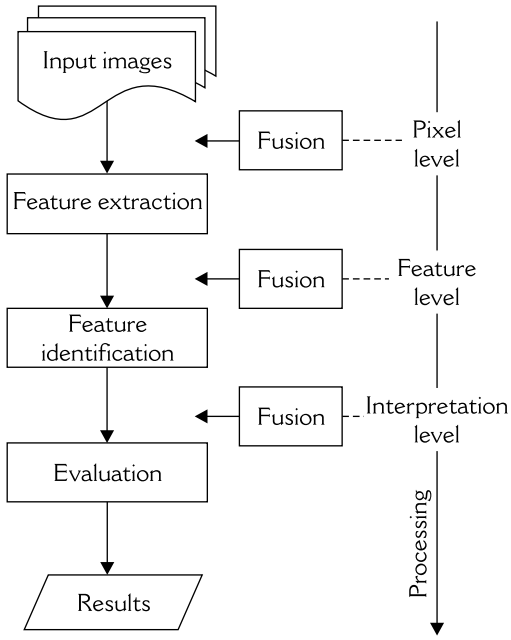

Figure 1 Processing level of data fusion
Source: Adapted from Pohl and van Genderen (1998).

- multisensor for spatial, eg, Landsat/MODIS (Moderate Resolution Imaging Spectroradiometer) (Gao *et al*., 2006);
- multisensor in single date, eg, ERS-1/ERS-2 (Guyenne, 1995);
- remote sensing data with ancillary data, eg, terrain data (Carpenter *et al*., 1997).

b Purpose of data fusion: Data fusion is used to combine multisource image using certain fusion algorithms. It can integrate disparate and complementary data to improve image resolution in spatial, temporal or/and spectral aspects, and consequently to lead to more accurate data (Keys *et al.*, 1990) and increased utility (Rogers and Wood, 1990). More specifically, the data fusion is applied to digital imagery in order to:

- sharpen images (Ranchin and Wald, 2000);
- improve co-registration (Leprince *et al.*, 2007);
- provide stereo-viewing capabilities for stereophotogrammetry (Bloom *et al.*, 1988);
- complement data sets for improving classification accuracy (Chanussot *et al.*, 2006);
- detect temporal change (Gao *et al.*, 2006);
- substitute missing information (eg, cloud issue in MS image, or shadows in radar image) in one image with signals from another sensor image (Hegarat-Mascle *et al.*, 1998).

The following points describe the purpose in more detail.

(1) *Pansharpening*. High-resolution panchromatic imagery is fused with low-resolution multispectral image data. These synthetic images looks like multispectral (MS) images observed with a sensor at the higher resolution (Ranchin and Wald, 2000).

(2) *Improvement of co-registration*. The input images might come from multiple platforms, multiple sensors on board the same instrument, ancillary data sources, and so on. This situation usually requires the user to work on multisensor or multitemporal data sets simultaneously. The first problem encountered is co-registration, which remains a crucial step in numerous applications and still generates much critical attention (Wong and Clausi, 2007).

(3) *Provide stereo-viewing capabilities for stereophotogrammetry*. VIR/VIR (different spatial resolution), SAR/SAR (multiple incidence angles), and VIR/SAR were successfully fused to create stereo data sets. Bloom *et al*. (1988) demonstrated the stereophotogrammetry with combined SIR-B (Shuttle Imaging Radar-B) and Landsat TM images, and Gelautz *et al*. (2003) derived and compared radar stereo and interferometric DEMs (digital elevation models) using a Radarsat stereo pair, and Radarsat and ERS-2 interferometric data.

(4) *Improvement of classification accuracy*. Images from microwave and optical sensors offer complementary information that helps in discriminating the different classes.
(5) *Detection of temporal change*. For example, Landsat's temporal resolution is 16 days, which is too long for detecting the vegetation change in temporal scale. Because MODIS has a daily revisit capability, fusion of Landsat and MODIS can help resolve this problem.
(6) *Substitution of missing information*. The images acquired by satellite sensors are influenced mainly by the carrier frequency of the electromagnetic waves. It is well known that the optical imagery is subject to interference from clouds, and thus the shadows of the clouds block the interpretability of the imagery. Radar imagery, on the other hand, suffers from severe geometric distortions and speckle due to its side-looking geometry. Therefore there is a big need and prospect to combine different images acquired by the same or by different instruments.

III Possible sensors and methods for the challenges and opportunities

Newly advanced sensors and methods are increasing the probability of tackling the aforementioned problems, and providing great opportunities for new interpretative research and applications.

1 Possible sensors for large-area habitat mapping

As mentioned above, the limitations of Landsat suggest that alternative imagery should be tested for its suitability in wildlife habitat mapping. Currently available satellite-based imagery can be divided into three categories based on its relationship between scale and spatial resolution: low spatial resolution imagery (optical applications are most suitable for studying phenomena that vary over hundreds or thousands of metres (small scale), eg, NOAA (National Oceanic and Atmospheric Administration) AVHRR (Advanced Very High Resolution Radiometer), EOS (Earth Observing System) MODIS, and SPOT (Satellite Pour l'Observation de la Terre) VEGETATION sensor data); medium spatial resolution imagery (optical applications are most suitable for studying phenomena that vary over tens or hundreds of metres (medium scale), eg, Landsat, SPOT, IRS (Indian Remote Sensing satellite) sensor data); and high spatial resolution imagery (optical applications are suitable for studying phenomena that vary over centimetres to metres (large scale), eg, aerial remote sensing platforms, IKONOS, and QUICKBIRD-2 sensor data; Franklin and Wulder, 2002).

Among these three categories of satellite imagery, Franklin and Wulder (2002) have pointed out that medium spatial resolution satellite imagery might be suitable for large-area land-cover mapping. Medium spatial resolution imagery can provide detailed information to compare with coarse-resolution imagery, and simultaneously guarantee large enough image size for large-area mapping to high-resolution imagery. The challenge on Landsat-series data may be avoided if information from satellites such as those listed in Tables 1 and 2 are tested and proven capable of delivering the information required. Figure 2 links the optical imagery properties listed in Table 1 to their specific habitat applications. Taking land-cover classification as an example, spatial and spectral resolution can guarantee sufficient tone, size, shape, and texture information for classification with required accuracy. In addition, image size can determine whether the image will cover the total study area. However, spatial resolution and image size have a negative relationship, which means that high spatial resolution corresponds to a small image size and vice versa. Therefore, users have to compromise according to their objectives. For radar sensors, polarization is an exclusive property compared to optical sensors. It also provides useful information for a variety of applications (Table 3).

Table 1 Possible medium-resolution optical sensors

Medium resolution sensors	Spatial resolution (m)[a]	Swath (km)	Spectral resolution (nm)	Temporal coverage	Revisit (day)
IRS-P6 (Resourcesat-1) (LISS III)	23.5	141	520–1700	2003 to Present	24
SPOT 4 (HRVIR)	20	60	500–1750	1998 to Present	1–3
SPOT 5 (HRG)	10 (MS); 20 (SWIR)	60	500–1730	2002 to Present	1–3
CBERS-1 and -2	20	120	450–890	1999/2003 to Present	3
Terra (ASTER)	15	60	530–1165	1999 to Present	16
EO-1 (ALI)	10 (Pan); 30 (MS)	37	433–2350	2000 to Present	16
ALOS (AVNIR-2)	10	70	420–890	2006 to Present	2
DMC (SLIM-6)	22/32	600	520–990	2002 to Present	1

[a]MS = multispectral; SWIR = shortwave infrared; Pan = panchromatic.

Table 2 Possible radar sensors

Sensors	Spatial resolution (m)	Footprint (km^2)	Polarization	Temporal coverage	Revisit (day)
TerraSAR-X (X-band)	18	100*150	Single VV or HH	2007 to Present	2.5
ERS-2 (C-band)	25	100*100	VV	1995 to Present	12–20
Radarsat-1 (C-band)	25/30	100*100/ 150*150	HH	1995 to Present	1–3
Radarsat-2 (C-band)	26.8–18.0*24.7/ 40.0–19.2*24.7	100*100/ 150*150	Single (HH or VV or HV or VH) or Dual ((HH + HV) or (VV + VH))	2007 to Present	1.5
ALOS PALSAR (L-band)	44-7/88-14	40-70* 40-70	(HH or VV) or (HH+HV or VV+VH)	2006 to Present	2
ENVISAT ASAR (C-band)	30	100*100	(HH or VV) or (VV+HH or HH+HV or VV+VH)	2002 to Present	4

Table 3 Radar polarization and potential application (adapted from Radarsat-2 Information, 2009a)

Polarization	Application		
	Forest	Hydrology	Agriculture
Single	Fire-scar mapping; low biomass estimation	Soil moisture; wetland detection; shoreline mapping	Crop canopy volume and structures; land use
Dual	Clear-cut mapping	Mapping of surficial deposits and rock units; tidal and near shore mapping	Crop discrimination
Quad	Stand age retrieval; forest structure estimation	Snow; wetland classification	Crop condition mapping; crop yield mapping

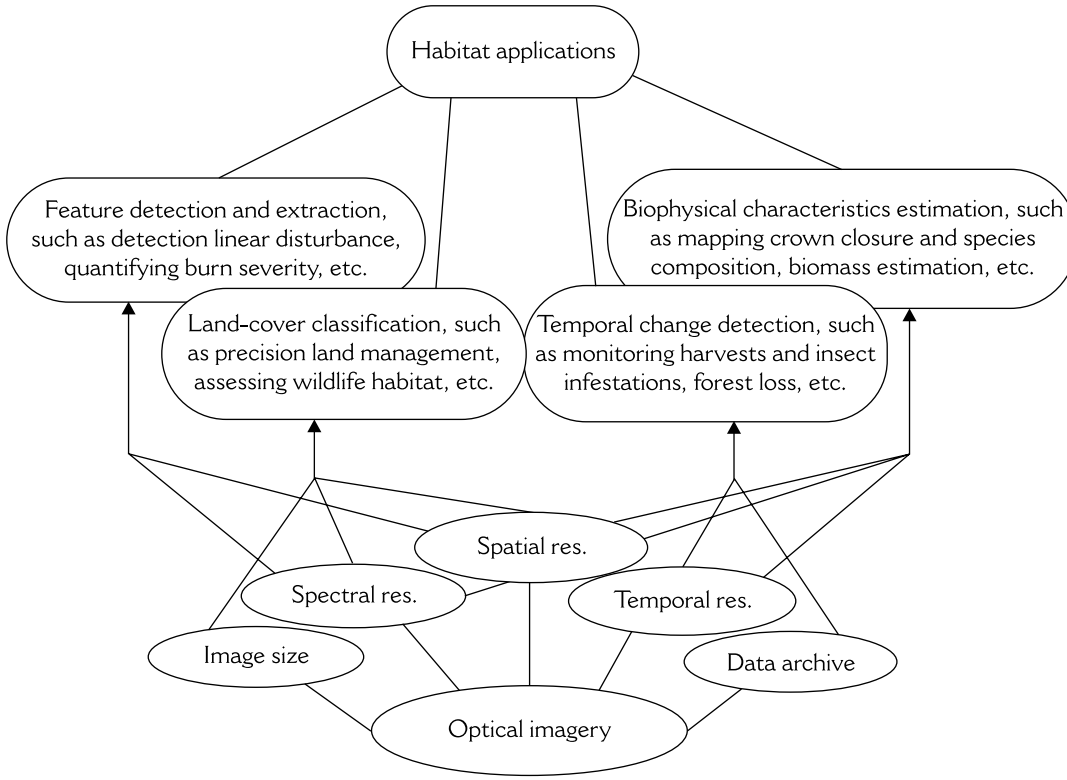

Figure 2 Linkage of optical imagery properties and habitat applications

a DMC (SLIM-6): The Disaster Monitoring Constellation (DMC) was designed as a proof of concept constellation (Table 4), capable of obtaining multispectral images of any part of the world every day. Surrey Linear Imager – 6 Channels (SLIM-6) is a dual bank linear push broom imager utilizing the orbital motion of the DMC platform to capture radiation reflected from the Earth's surface (Crowley, 2008). SLIM-6 has three bands, ie, NIR (0.77–0.90 μm), Red (0.63–0.69 μm), and Green (0.52–0.60 μm), which are equivalent to Landsat TM or ETM+ band 4, band 3, and band 2, respectively. The combination of the above sensor characteristics can support DMC imagery to be used for extensive practical applications. For example, its 32 m spatial resolution and three spectral bands are analogous to the Landsat TM and ETM+ data, which allows image users to generate comparable remote sensing products used in existing habitat mapping and ecological models. A one-day temporal resolution can satisfy the application of detecting rapid surface changes such as crop-growth monitoring and detecting intra-seasonal ecosystem disturbance. Meanwhile, the high temporal resolution also promotes acquisition of good-quality imagery with limited cloud contamination. The sensor has been used in many applications including forest, agriculture, land-cover and habitat mapping, and flood or fire monitoring. It is especially suitable for large area land-cover mapping due to the 600 km swath width. The cost of purchasing DMC data ranges from 0.018 to 0.164 US dollars per km^2 depending on desired data types (DMC International Imaging Ltd, 2008). The further exploitation of DMC data likely provides an appropriate data source to traverse the coming Landsat gap.

Table 4 Disaster Monitoring Constellation (DMC) on orbit (adapted from DMC International Imaging Ltd)

Designation	Type	Imager	Launch
Alsat-1	DMC	32 m MS	2002
UK-DMC	DMC	32 m MS	2003
Nigeriasat-1	DMC	32 m MS	2003
Beijing-1	DMC+4	32 m MS/4 m Pan	2005
Deimos-1	DMC	22 m MS	2008
UK-DMC2	DMC	22 m MS	2008

MS = multispectral; Pan = panchromatic.

b ALOS PALSAR and Radarsat-2: Radar, the acronym of radio detection and ranging, is based on the transmission of long-wavelength microwaves (eg, 3–25 cm) through the atmosphere and then recording the amount of energy backscattered from the terrain (Jensen, 2007). Radar remote sensing uses the microwave portion of the electromagnetic spectrum, from a frequency of 0.3 GHz to 300 GHz, or, in wavelength terms, from 1 m to 1 mm (Canada Centre for Remote Sensing, 2008). Most remote sensing radars operate at wavelengths from 0.5 cm to 75 cm (Canada Centre for Remote Sensing, 2008). The microwave frequencies have been arbitrarily assigned to different bands which are identified by letter. The most popular of these bands for use by imaging radars are included in Table 5 (Jensen, 2007). The capability to penetrate through cloud or into a surface layer is increased with longer wave-lengths, eg, L-band radar sensors have better penetration than the C-band sensors. However, radars operating at wavelengths greater than 2 cm are not significantly affected by cloud cover (Canada Centre for Remote Sensing, 2008). Jensen (2007) summarized the primary advantages of radar as follows:

(1) certain microwave frequencies will penetrate clouds, allowing all-weather remote sensing;
(2) it allows synoptic views of large areas for mapping from 1:10,000 to 1:400,000 and satellite coverage of cloud-shrouded countries is possible;
(3) coverage can be obtained at user-specified times, even at night;
(4) it permits imaging at shallow look angles, resulting in different perspectives that cannot always be obtained using aerial photography;
(5) it senses in wavelengths outside the visible and infrared regions of the electromagnetic spectrum, providing information on surface roughness, dielectric properties, and moisture content.

The Phased Array type L-band Synthetic Aperture Radar (PALSAR) on board Advanced Land Observing Satellite (ALOS) is an enhanced version of the JERS-1 SAR (Japanese Earth Resources Satellite), launched in January 2006 by the Japanese Aerospace Exploration Agency (Rosenqvist *et al.*, 2007). It is a fully polarimetric instrument, which operates in L-band with 1270 MHz (23.6 cm) centre frequency and 14 and 28 MHz bandwidths. PALSAR operates in single-polarization (HH or VV), dual-polarization (HH+HV or VV+VH), or quad-polarization mode, and the nominal ground resolution is ~10 and ~20 m in the single- and dual-polarization modes, respectively, and ~30 m in quad-pol mode (Rosenqvist *et al.*, 2004). It can also operate in a coarse, 100 m, resolution ScanSAR mode, with single-polarization (HH or VV) and 250–350 km swath width (Rosenqvist *et al.*, 2004).

Table 5 Bands for use by imaging radars

Band designations (common wavelengths)	Wavelength (cm)	Frequency (GHz)	Typical sensors
X (3.0 and 3.2 cm)	2.4–3.8	12.5–8.0	CV-580 SAR
C (5.6 cm)	3.9–7.5	8.0–4.0	ERS-1 and RADARSAT
S (8.0, 9.6, 12.6 cm)	7.5–15.0	4.0–2.0	Almaz[a]
L (23.5, 24.0, 25.0 cm)	15.0–30.0	2.0–1.0	SEASAT and PALSAR
P (68.0 cm)	30.0–100	1.0–0.3	NASA/JPL AIRSAR

[a]The Almaz programme was a series of military space stations (or 'Orbital Piloted Station' – OPS) launched by Russia.

Until now, PALSAR was the only available spaceborne L-band SAR with quad-pol mode to exist. Surface features can be readily discriminated if radar wavelength is matched to the size of the features (Canada Centre for Remote Sensing, 2008). Consequently, the L-band is much better in geology mapping, and the corresponding low frequency is better for detecting water under closed canopies (Canada Centre for Remote Sensing, 2008). In theory, quad-pol has more inherent information per pixel than dual- and single-pol, and so quad-pol data should produce more accurate products. PALSAR images have been successfully used for scientific researches on, for example, earthquake (eg, Lubis and Isezaki, 2009; Jin and Wang, 2009), ice sheet (eg, Rignot, 2008), hydrology (eg, Paillou *et al.*, 2009), and soil science (eg, Takada *et al.*, 2009).

RADARSAT-2 (R-2) is the follow-on mission to RADARSAT-1 (R-1) designed to assure continuity of the supply of radar data, launched in December 2007 by the Canadian Space Agency (CSA) and MacDonald Dettwiler and Associates Ltd (MDA). However, the R-2 represents a significant evolution from R-1 in aspects of spatial resolution, polarization, and look direction (Table 6). With these advanced features, it is believed that R-2 can be used in many relevant application areas, such as improving resource management operations in the areas of ice and oceans, agriculture, geology, and hydrology, and supporting the global effort to improve environmental quality through environmental planning, assessment, and management (Morena *et al.*, 2004). More specific to applications in forestry, R-2's array of beam modes and polarimetric capabilities is likely to provide significant steps forward in the detection of structural differences between forests, and offer greater potential for burn mapping. For example, ultra-fine beam mode provides increased accuracy of boundary placement; HV or VH single-pol likely provides the best potential for burn mapping since it is sensitive to structural damage incurred by the forest canopy (Radarsat-2 Information, 2009a). High-resolution data from RADARSAT-2, such as 3 m ultra-fine mode data or 12 m fine quad-pol mode data, offers the potential to improve forest-type mapping using textural analysis (Radarsat-2 Information, 2009a). In the context of geology, R-2's ultra-fine resolution and fully polarimetric capabilities can provide benefits such as more detailed mapping of terrain features or fine geological structures, better identification of structural features and improved discrimination of different geologic units (Radarsat-2 Information, 2009a).

2 Methods for detection and removal of clouds and their shadows

In general, cloud cover is the unwanted information in optical images (Tseng *et al.*, 2008). In this context, if complementary information can be found to replace cloud- and cloud

Table 6 RADARSAT-2 innovations (adapted from Radarsat-2 Information, 2009b)

Items	Characteristics	Specifics
Spatial resolution	3–100 m	• Suite of spatial resolution options accommodates a wide range of applications • Ultra-fine beam will improve object detection and recognition
Polarization	HH, HV, VV and VH	• Better discrimination of various surface types and improved object detection and recognition
Look direction	Routine left- and right-looking operation	• Increased revisit time for improved monitoring efficiencies • More responsive to user requests • Antarctic mapping mission fully integrated

shadow-contaminated areas, the problem will be resolved to generate cloud-free images or map products. Multitemporal and radar images are considered a good choice to provide the complementary information (Hegarat-Mascle *et al.*, 1998; Wang *et al.*, 1999; Tseng *et al.*, 2008). The general steps of producing cloud-free images include image pre-processing (co-registration, correction of brightness, and image enhancement), detection of clouds and cloud shadows, and removal of clouds and their shadows (replacement). Many approaches have been developed to tackle obstacles at every step, but here we focus on reviewing the methods of detection and the removal of clouds and their shadows.

a Detection of clouds and their shadows: Simpson and Stitt (1998) developed the pixel-by-pixel cross-track geometry of the scene and image analysis methods to detect cloud shadow in daytime AVHRR scenes over land. These methods are not suitable for removing clouds and their shadows in other satellite imagery (Meng *et al.*, 2009). However, the most frequently used method is one based on a threshold, of which the values may vary for images acquired at different time (Meng *et al.*, 2009). Chen (2001) stated clouds and their shadows can be detected using thresholds obtained from all five AVHRR (Advanced Very High Resolution Radiometer) channels as well as systematic mathematical expressions. The five channels involve the use of surface reflectance (channels 1 and 2) and thermal (channels 3, 4, and 5) data. Cloud detection is based on the characteristic that clouds are generally bright in the visible spectrum (channel 1) and/or cold in the infrared spectrum (channel 2) (Gutman, 1992), and highly reflective in channel 3 and/or relative cold in channels 4 and 5 (Yamanouchi and Kawaguchi, 1992). Chen (2001) tested different thresholds for the detection of clouds and their shadows in AVHRR imagery, and used the thresholds of 0.27 for channel 1, 223 K for channel 4 and 0.8–1.6 for the ratio of channel 2 reflectance, to channel 1 reflectance. Finally, the contaminated pixels are classed into thick clouds, thin clouds, optical cirrus, cloud edges and cloud shadows according to their impacts on normalized difference vegetation index (NDVI). However, thermal bands are not available for many of the popular sensors, such as SPOT and IRS.

With Landsat imagery, Automatic Cloud Cover Assessment (ACCA) can detect clouds over most of the earth's surface by their high albedo in the visible spectrum and by their cold temperatures (Choi and Bindschadler, 2004). However, it is prone to mix up clouds and ice sheets because both

targets are bright and temperature inversions in the atmosphere above the ice sheets are common. This leaves the surface colder than the clouds (Choi and Bindschadler, 2004). Thus, an approach using the normalized difference snow index (NDSI) was developed by Choi and Bindschadler (2004). Besides cloud detection, Wang *et al.* (1999) suggested it is difficult to detect the shadow regions because of the similar brightness values between shadows and their neighbours or some other regions. Therefore, Wang *et al.* (1999) applied wavelet transforms to detect shadow regions, because shadows reduced the local contrasts of the image, and the wavelet coefficients can measure the local contrasts of the image at different scales.

In addition, Griffin *et al.* (2003) developed a cloud-cover algorithm for application to EO-1 (Earth Observer-1) Hyperion hyperspectral data. The algorithm successfully discriminated clouds from surface feature such as snow, ice, and desert sand only utilizing six bands in the reflected solar spectral regions. Tseng *et al.* (2008) used the linear spectral unmixing method (LSU) to extract all of the cloud-cover pixels, but it cannot handle thin clouds and cloud shadow, and often confuses bright land surfaces as clouds.

b Removal of clouds and their shadows: Adapted from the Tseng *et al.* (2008) research, the methods of removal can be categorized into four general classes according to the source of complementary information: (1) using image statistical information to interpolate or treat the cloud as noise to remove (eg, Rossi *et al.*, 1994; Feng *et al.*, 2004); (2) using multispectral images to fuse and generate the cloud-free images (eg, Wang *et al.*, 2005); (3) using multitemporal images to fuse and generate the cloud-free images (eg, Wang *et al.*, 1999; Tseng *et al.*, 2008; Meng *et al.*, 2009); and (4) because radar images are not affected by clouds, using radar images can restore the cloud-covered area (eg, Thanh *et al.*, 2008).

An example from the first category, proposed by Feng *et al.* (2004), was called an improved homomorphism filtering method. This was based on the statistical characters of image information to remove cloud. Instead of filtering in the frequency field, it isolates the low-frequency component of the image representing cloud information by calculating neighbourhood averages in the spatial field. However, this method readily leads to the confusion of bright land-cover area and clouds; moreover, theoretically the denoising methods cannot completely recover the land covers blocked by the clouds (Tseng *et al.*, 2008). An example from the second category, proposed by Wang *et al.* (2005), encounters cloud contamination in all bands of multispectral images; in such a case, the clouds are also treated as noises and the similar results to these of the first-category methods are acquired (Tseng *et al.*, 2008). As a result, neither class of methods is likely to become mainstream in use.

More effort has gone into generating cloud-free composite images based on multitemporal methods. Wang *et al.* (1999) developed a scheme to remove clouds and their shadows from remotely sensed images of Landsat TM. The scheme uses the image fusion technique to automatically recognize and remove contamination of clouds and their shadows, and integrate complementary information into the composite image from multitemporal images. Tseng *et al.* (2008) generated cloud-free mosaic images from multitemporal SPOT images based on multidisciplinary methods, such as the multiscale wavelet-based fusion method. Meng *et al.* (2009) proposed an efficient approach, called closest spectral fit. This technique can avoid the spectral inconsistency between the substitution and original image, and it does not depend on the areas, the thickness, and the density of clouds and cloud shadows in the images.

The use of radar images to remove clouds and their shadows has rarely been studied,

largely because optical and radar sensors fall into totally different genera (Jensen, 2007), which may result in more complicated processing than using multitemporal methods. But the multitemporal methods require that cloudy areas in the base image should be cloud-free in the complementary image. Frequently it is impossible or extremely difficult to obtain a cloud-free complementary image, especially in tropical or cloud-prone areas. Most importantly, the Landsat imagery, with its low temporal resolution (16 days) is further limited when research objects change dramatically in a short time period. Hence, radar imagery has exclusive advantages in addressing the cloud issue when compared with multitemporal optical imagery. Thanh *et al.* (2008) achieved promising results on cloud removal of optical image using SAR data.

3 Fusion techniques of optical and radar imagery

Optical and radar image fusion is always at the leading edge of remotely sensed data fusion. The relevant technology has become progressively more systematic. Figure 3 indicates the outline of fusion between optical and radar images. Generally, system error will be corrected by the providers of the data, but the data need to be subject to further radiometric processing using a filter or other algorithms. Radar images have a strong 'salt and pepper' phenomenon (ie, speckle). Therefore, speckle reduction is an elementary operation in processing, and some remote sensing professionals suggest first reducing speckle before geocoding (Dallemand *et al.*, 1993). Optical imagery acquisition is strongly influenced by atmospheric conditions and therefore needs correction. The next step

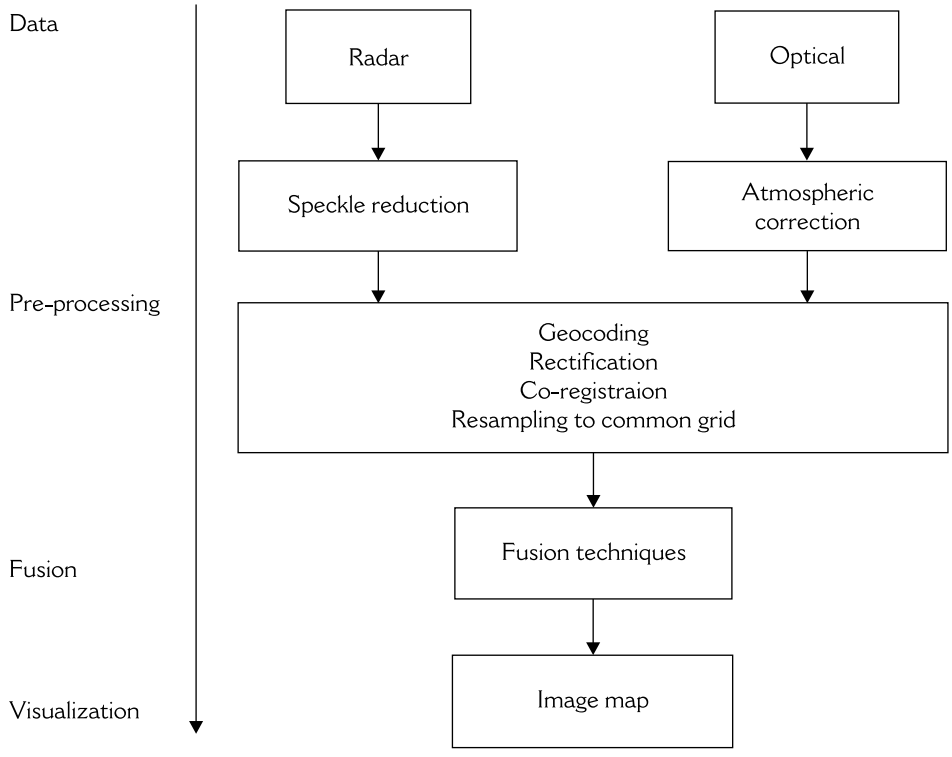

Figure 3 Outline of optical and radar image fusion

Source: Adapted from Pohl and van Genderen (1998).

is geocoding, or co-registration, because the techniques are sensitive to misregistration (Pohl and van Genderen, 1999). Data can then be fused according to the fusion techniques described below. However, if the image data are very different in spatial resolution, resampling from low to high resolution causes the data to appear blocky (Pohl and van Genderen, 1999). Therefore, Chavez (1987) recommended using a smoothing filter before image fusion – any spatial or spectral enhancement related to the application prior to image fusion will benefit the resulting fused image (Pohl and van Genderen, 1999).

In general, the fusion techniques can be categorized into two classes (Pohl and van Genderen, 1998): (1) colour-related techniques, such as colour composites (RGB), intensity-hue-saturation (IHS); (2) Statistical or numerical methods, such as principal component analysis (PCA), band combinations using arithmetic operators and others. Table 7 indicates the most successful techniques for fusing images from Landsat, SPOT, ERS-1 and JERS-1 – Japanese Earth Resources Satellite; Pohl and van Genderen, 1999). Besides the typical techniques, more new techniques focus on the modelling and combination of fusion algorithms with the development of sensors and computation. For example, Farah *et al*. (2008) presented a semi-automatic approach based on case-based reasoning (CBR) to fuse images from ERS-2 and SPOT 4, and obtained encouraging results. Corbane *et al*. (2008) developed an algorithm consisting of a completely unsupervised procedure for processing pairs of co-registered SAR/optical images. Waske and van der Linden (2008) proposed a joint classification of multiple segmentation levels from multisensor imagery using SAR and optical data, and implemented this method based on a support vector machine (SVM). Garzelli (2002) proposed a method aiming to generate an integrated map which selects specific information from SAR data to be injected into the optical data based on

Table 7 Typical techniques testing on fusion from optical and radar sensors

Categorization	Techniques	Results
Colour-related	RGB	Simple, and does not require CPU time-intensive computations. RGB overlay protects the contribution from optical imagery from being greatly affected by speckle from SAR.
	IHS	With the capability of allocating data from the SAR to cloud-cover areas without having to identify the clouds at an earlier stage, but will reduce spatial detail.
Statistical or numerical	Band combinations	Improve the interpretation of the SAR data, but depend very much on the appearance and content of the SAR image. Do not solve the cloud-cover problem.
	Brovey transform	Successfully combine spectral information from the VIR with texture from the SAR data.
	PCA	Principal component SAR images show potential for topographic mapping, especially for the 3D impression of topography and change detection.

the wavelet which is not referred to in classical IHS or PCS (Principal Component Substitution).

IV Application issue – landscape analysis and remote sensing

Landscape analysis refers to accurately quantifying landscape pattern, which has been commonly used in applications of resource management, environmental conservation and impacts of anthropogenic activity. A large number of metrics have been developed for quantifying landscape pattern since the seminal paper by O'Neill *et al.* (1988). Advances in remote sensing technologies have provided practical means for classified thematic maps which are the key inputs for most studies on landscape pattern analysis (Shao and Wu, 2008).

However, before using classification maps to calculate landscape metrics, classification accuracy should be assessed via analytically comparing satellite sensor derived products (eg, land cover) to reference data, which is presumed to represent the target value (Justice *et al.*, 2000). This is because the classification errors will be carried over or even propagated in subsequent landscape pattern analysis (Fang *et al.*, 2006; Shao and Wu, 2008).

1 Accuracy assessment

Accuracy assessment is a critical step in analysing any map created from remotely sensed data. Quantitative accuracy assessment is implemented to identify and measure map errors (Congalton and Plourde, 2002). The most widely used approaches in accuracy assessment are to calculate RMSE (see below) and to create an error matrix. Before the assessment, one needs to learn about the source of errors (Powell *et al.*, 2004). Besides the error gained from the method itself, other sources of errors include registration errors, processing errors, interpretation errors, and sampling errors, all of which will affect the accuracy of results (Lu and Weng, 2007).

RMSE is root mean square error, also called standard deviation, which is a measure of positional accuracy that encompasses both the effects of bias and random error. Because of the simplicity of RMSE calculation, it has long been utilized in accuracy assessments of remote sensing products (eg, Cohen *et al.*, 2003; McDermid, 2005; Xu *et al.*, 2005). The error matrix is currently at the core of the accuracy assessment literature (Foody, 2002). Congalton and Plourde (2002) stated that in order to correctly generate an error matrix the following factors need to be considered: (1) reference data collection; (2) classification scheme; (3) sampling scheme; (4) spatial autocorrelation; and (5) sample size and sample unit. Afterwards, one can calculate overall accuracy, user's accuracy (commission error), producer's accuracy (omission error), and kappa coefficient. The meaning and computation methods of an error matrix can be found in previous literature such as Congalton and Plourde (2002) and Foody (2002).

2 Landscape pattern analysis using remote sensing data

Landscape pattern is spatially correlated and scale-dependent (Wu, 2004). In particular, any measures of spatial heterogeneity in the landscape pattern, or of patch characteristics via metrics will be scale-dependent (Wu and Hobbs, 2002; Li and Wu, 2004; Wu, 2004). The term 'scale' may refer to any one or combinations of several concepts, including grain (spatial resolution), extent (geographic), lag (or spacing), and cartographic ratio (Wiens, 1989; Lam and Quattrochi, 1992; Wu, 2004), but the most commonly examined scales are grain or extent (Urban, 2005; Kent, 2007), which have previously been described as the 'Modifiable Areal Unit Problem' (MAUP) in Geographic Information Systems (GIS) (Kent, 2007). For remotely sensed data, grain and extent relate to image spatial resolution and footprint (image size), respectively. It is straightforward to deal with the

extent issue via seamless image mosaicing. Accordingly, we focus on discussing the relationship of landscape metrics and image spatial resolution, and landscape metrics and thematic resolution. Furthermore, confronted with the limitations and uncertainties of Landsat-series data, it is important to examine what should be done at the application level. For instance, most ecological or resource-management models are Landsat-dependent, and if they must use other imagery to produce the mapping products it will result in incompatibility, or even conflict with derived models because of distinct spectral and spatial resolution.

a Landscape metrics and spatial resolution: Benson and MacKenzie (1995) examined the effects of grain size (spatial resolution) on landscape parameters characterizing spatial structure, ie, whether structural parameters remain constant from 20 m to 1100 m of grain size, and whether aggregation algorithms permit extrapolation within this range. Landscape parameters were used to quantify spatial structure, including percentage of water, number of lakes (patches), average lake area and perimeter, fractal dimension, and three measures of texture (homogeneity, contrast, and entropy). Results indicate that most measures were sensitive to changes in grain size. However, it was found that two texture measures were relatively invariant with grain size – homogeneity and entropy. The aggregation of the results indicated that extrapolated values closely approximated the actual sensor values, and that interpolation between the grain sizes of different satellite sensors is possible when an approach involving an aggregation of pixels is applied.

However, considerable differences between aggregated values and actual sensor values were found by Saura (2004), who examined the effect of spatial resolution on six common fragmentation indices that are being used within the Third Spanish National Forest Inventory. Number of Patches (NP), Mean Patch Size (MPS), and Edge Length (EL) indicated that the aggregated values produced clearly more fragmented patterns than actual sensor ones. Different aggregation algorithms were tested in the context of forest fragmentation estimates across various spatial scales (Garcia-Gigorro and Saura, 2005). Thirty-metre Landsat-TM forest data were transferred to 188 m IRS-WiFS (Indian Remote Sensing Satellite-Wide Field Sensor) and compared with actual WiFS data. Sensor point spread function was found to greatly improve comparability of forest fragmentation indices. However, a poor performance of power scaling laws was observed at finer spatial resolutions, and accordingly Garcia-Gigorro and Saura (2005) suggested that the true accuracy and practical utility of these scaling functions may have been overestimated in previous literature. In addition, the sensitivity of each of the indices varied with the gradient of spatial resolution. But Cain *et al.* (1997) conducted a multivariate analysis of pattern metrics, and pointed out that measures of land-cover diversity, texture, and fractal dimension were more consistent than measures of average patch shape or compaction among the land-cover maps. Wu *et al.* (2002) summarized the responses of the 19 landscape metrics that fell into three general categories when calculated at the landscape level: Type I metrics showed predictable responses with changing scale, and their scaling relations could be represented by simple scaling equations (linear, power-law, or logarithmic functions); Type II metrics exhibited staircase-like responses that were less predictable; and Type III metrics behaved erratically in response to changing scale, suggesting no consistent scaling relations. Therefore, if metrics fall within category Type I they can be readily and accurately extrapolated or interpolated across spatial scales, whereas if they fall in Type II or Type III categories more explicit consideration of idiosyncratic details are required for successful scaling.

Proportion errors cannot be avoided when land-cover classification data are aggregated

to coarser scales. Moody and Woodcock (1995) tested two statistical models, multiple-linear and tree-based regression techniques, to assess relationships between landscape spatial pattern and errors in the estimates of cover-type proportions. Results from a multiple-linear regression model suggest that as patch sizes, variance/mean ratio, and initial proportions of cover types increase the proportion error moves in a positive direction and is governed by the interaction of the spatial characteristics and the scale of aggregation. However, the linear model does not explain the different directions of the proportion error. A regression tree model provided a much simpler fit to the complex scaling behaviour through an interaction between patch size and aggregation scale. The understanding of proportion errors can help correct land-cover proportion estimates.

b Landscape metrics and thematic resolution: The thematic resolution of remote sensing products is determined by the applied land-cover classification scheme. This represents the amount of detailed geospatial information, and influences on the various aspects of landscape classification and the relevance of the derived pattern attributes to particular ecological questions (Buyantuyev and Wu, 2007). Changing the thematic resolution of categorical maps may often alter the number of classes and their spatial pattern, thus resulting in differences in landscape metrics (Buyantuyev and Wu, 2007). Many research results have proven that thematic resolution had significant effects on most of the landscape metrics, such as Huang *et al*. (2006), Buyantuyev and Wu (2007), and Castilla *et al*. (2009). For example, Buyantuyev and Wu (2007) stated that three general response patterns emerged: increased, decreased, and little change. Most of the changes appear either linear or similar to a power-law. Additionally, Huang *et al*. (2006) pointed out that at lower class numbers, landscape metrics were most sensitive to increasing classification detail.

c Solutions to the Landsat-gap on application level: It is necessary to generate Landsat-like classification maps using other alternative satellite images (eg, SPOT, DMC or radar images), if the expected Landsat-gap happens. It is of vital importance for the subsequent landscape pattern analysis or relevant ecological models to be based on Landsat classification maps. As discussed, scale issues caused by spatial, thematic, and spectral resolutions have a significant effect on classification, and consequently the calculation of landscape metrics. In general, three promising solutions are suggested to partly address this issue: (1) select approximate 30 m spatial resolution alternatives (eg, DMC 32 m multispectral images); (2) adjust the procedural parameters of classification; (3) apply scaling relationships between landscape metrics and grain size to set up the model. The following points provide detailed information regarding these solutions.

- *Solution 1*. Landscape metrics are calculated based on classification maps with certain grain size. DMC imagery has 32 m spatial resolution, and three bands which are equivalent to Landsat TM or ETM+ bands 2, 3 and 4. It is considered to be the closest sensor to Landsat TM or ETM+, and consequently it is likely to generate comparable classification maps.
- *Solution 2*. Franklin *et al*. (2009) tested the capability of SPOT and ASTER for replacing Landsat in an operational environment. An approach based on Definiens' Developer (also called eCognition; Definiens AG, 2008) was developed to diminish the dissimilarity between SPOT- and ASTER-based and Landsat-based classification as far as possible. The results indicated that if set Scale = 55, Shape = 0.2, and Compactness = 0.2 to

segment SPOT imagery, and 20, 0.2, 0.2 to segment ASTER imagery in the process of object-oriented classification, the minimum dissimilarity could be obtained. Herein, the 'Scale' in Definiens' Developer is a unitless parameter that determines the size of objects. This means that pixels are merged if their values are within a user-defined threshold (Elmqvist *et al.*, 2008). 'Shape' represents the shape information considered in the segmentation and is defined by the compactness and smoothness heterogeneity of objects (Elmqvist *et al.*, 2008). 'Compactness' equals the ratio of the perimeter of an object and the square root of the number of pixels forming that image object (Benz *et al.*, 2004).

- *Solution 3*. The scaling relationships between landscape metrics and grain size, ie, how pattern metrics change with scale in real landscapes of different kinds, have been revealed by many researchers, such as Benson and MacKenzie (1995), Cain *et al*. (1997), Wu *et al*. (2002), Saura (2004), and Wu (2004). Wu *et al*. (2002) grouped the effects of changing grain size into three general types: Type I, simple scale functions; Type II, staircase pattern; Type III, unpredictable behaviour. Twelve of the 19 landscape metrics we examined belonged to Type I, including the number of patches (NP), patch density (PD), total edge (TE), edge density (ED), landscape shape index (LSI), area-weighted mean shape index (AWMSI), area-weighted mean patch fractal dimension (AWMFD), patch size coefficient of variation (PSCV), mean patch size (MPS), square pixel index (SqP), patch size standard deviation (PSSD), and largest patch index (LPI). The relationships can help set up models to predict Landsat-based landscape pattern using alternatives, eg, SPOT imagery.

V Conclusions

Remote sensing provides significant information and plays a dominant role in large-area wildlife habitat mapping, although field data acquired by *in situ* methods are also indispensable for most studies. However, the limitations and uncertainties in remote sensing hinder the feasibility and reliability of remotely sensed data in large-area applications. Pioneering work has achieved promising results in addressing these issues, but a tremendous amount of research yet remains, especially regarding the limitations and uncertainties of Landsat-series data, clouds and cloud shadows in optical imagery, and landscape analysis and remote sensing. New optical and radar sensors, eg, DMC and Radarsat-2, may provide answers to the above questions. Future research should explore the applicability of these sensors in large-area wildlife habitat mapping, and develop reliable and efficient methods for supporting diverse environmental, ecological and resource management applications. Key areas to address are: fusing the complementary optical and radar images to improve classification accuracy; diminishing the difference of classified maps from diverse sensors on landscape pattern analysis via adjusting object-oriented classification parameters; developing a cloud classification scheme according to their impacts on ground objects; and applying radar to remove cloud contamination in optical imagery.

Acknowledgements

The authors would like to acknowledge the financial support of the Foothills Research Institute Grizzly Bear Program (FRIGBP) and the Department of Geography and Planning of the University of Saskatchewan.

References

Asner, G.P. 2001: Cloud cover in Landsat observations of the Brazilian Amazon. *International Journal of Remote Sensing* 22, 3855–62.

Benson, B.J. and **MacKenzie, M.D.** 1995: Effects of sensor spatial resolution on landscape structure parameters. *Landscape Ecology* 10, 113–20.

Benz, U.C., Hofmann, P., Willhauck, G., Lingenfelder, I. and **Heynen, M.** 2004: Multi-resolution, object-oriented fuzzy analysis of remote sensing data for GIS-ready information. *ISPRS Journal of Photogrammetry and Remote Sensing* 58, 239–58.

Bloom, A.L., Fielding, E.J. and **Fu, X.** 1988: A demonstration of stereophotogrammetry with combined SIR-B and Landsat TM images. *International Journal of Remote Sensing* 9, 1023–38.

Buyantuyev, A. and **Wu, J.** 2007: Effects of thematic resolution on landscape pattern analysis. *Landscape Ecology* 22, 7–13.

Cain, D.H., Riitters, K. and **Orvis, K.** 1997: A multi-scale analysis of landscape statistics. *Landscape Ecology* 12, 199–219.

Canada Centre for Remote Sensing 2008: Introduction to RADAR remote sensing. Retrieved 18 September 2009 from http://ccrs.nrcan.gc.ca/resource/tutor/gsarcd/downld_e.php

Carpenter, G.A., Gjaja, M.N., Gopal, S. and **Woodcock, C.E.** 1997: ART neural networks for remote sensing: vegetation classification from Landsat TM and terrain data. *IEEE Transactions on Geoscience and Remote Sensing* 35, 308–25.

Castilla, G., Larkin, K., Linke, J. and **Hay, G.J**. 2009: The impact of thematic resolution on the patch-mosaic model of natural landscapes. *Landscape Ecology* 24, 15–23.

Chander, G. 2007: Initial data characterization, science utility and mission capability evaluation of candidate Landsat mission data gap sensors (Draft pending final approval). *Landsat Data Gap Study, Technical Report – Version 1*, USGS and NASA. Retrieved 18 September 2009 from http://calval.cr.usgs.gov/documents/Landsat_Data_Gap_Studies/Landsat_Data_Gap_Study_%20Technical_Report6.pdf

Chanussot, J., Benediktsson, J.A. and **Fauvel, M.** 2006: Classification of remote sensing images from urban areas using a fuzzy possibilistic model. *IEEE Geoscience and Remote Sensing Letters* 3, 40–44.

Chavez, P.S. 1987: Digital merging of Landsat TM and digitized NHAP data for 1:24,000 scale image mapping. *Photogrammetric Engineering and Remote Sensing* 56, 459–67.

Chen, J.M. and **Black, T.A.** 1992: Defining leaf area index for non-flat leaves. *Plant, Cell and Environment* 15, 421–29.

Chen, P. 2001: An improved cloud detection algorithm for monitoring agricultural growing conditions with NOAA AVHRR in Texas. PhD thesis, Texas A&M University.

Choi, H. and **Bindschadler, R.** 2004: Cloud detection in Landsat imagery of ice sheets using shadow matching technique and automatic normalized difference snow index threshold value decision. *Remote Sensing of Environment* 91, 237–42.

Cohen, W.B. and **Goward, S.N.** 2004: Landsat's role in ecological applications of remote sensing. *Bioscience* 54, 535–45.

Cohen, W.B., Maiersperger, T.K., Gower, S.T. and **Turner, D.P**. 2003: An improved strategy for regression of biophysical variables and Landsat ETM+ data. *Remote Sensing of Environment* 84, 561–71.

Collingwood, A. 2008: Satellite image classification and spatial analysis of agriculture areas for land cover mapping of grizzly bear habitat. MS thesis, University of Saskatchewan.

Congalton, R.G. and **Plourde, L.** 2002: Quality assurance and accuracy assessment of information derived from remotely sensed data. In Bossler, J., editor, *Manual of geospatial science and technology*, London: Taylor and Francis.

Corbane, C., Faure, J.-F., Baghdadi, N. and **Petit, M.** 2008: Rapid urban mapping using SAR/optical imagery synergy. *Sensors* 8, 7125–43.

Crowley, G. 2008: DMC data product manual. *DMC International Imaging Ltd*. Retrieved 5 May 2009 from http://www.dmcii.com/index.html

Dallemand, J., Lichtenegger, J., Raney, R. and **Schumann, R.** 1993: Lecture notes. Rome: FAO Remote Sensing Centre.

Definiens AG 2008: Definiens Developer 7 – user guide. Retrieved 14 July 2009 from http://www.definiens.com/definiens-support-services_187_11_14.html

DMC International Imaging Ltd 2008: Price list. Retrieved 18 September 2009 from http://www.dmcii.com/pricing/DMCii_US_Prices_Oct2008.pdf

Draeger, W.C., Holm, T.M., Lauer, D.T. and **Thompson, R.J.** 1997: The availability of Landsat data – past, present, and future. *Photogrammetric Engineering and Remote Sensing* 63, 869–75.

Elmqvist, B., Ardo, J. and **Olsson, L.** 2008: Land use studies in drylands: an evaluation of object-oriented classification of very high resolution panchromatic imagery. *International Journal of Remote Sensing* 29, 7129–40.

Esche, H.A., Franklin, S.E. and **Wulder, M.A.** 2002: Assessing cloud contamination effects on K-means unsupervised classifications of Landsat data. *Proceedings of the 2002 IEEE International Geoscience and Remote Sensing Symposium (IGARSS '02)* 6, 3387–89.

Fang, S., Gertner, G., Wang, G. and **Anderson, A.** 2006: The impact of misclassification in land use maps in the prediction of landscape dynamics. *Landscape Ecology* 21, 233–42.

Farah, I.R., Boulila, W., Ettabaa, K.S., Solaiman, B. and **Ahmad, M.B.** 2008: Interpretation of multisensory remote sensing images: multiapproach fusion of uncertain information. *IEEE Transactions on Geoscience and Remote Sensing* 46, 4142–52.

Feng, C., Ma, J., Dai, Q. and **Chen, X.** 2004: An improved method for cloud removal in ASTER data change detection. *Proceedings of the IEEE International Geoscience and Remote Sensing Symposium (IGARSS '04)* 5, 3387–89.

Foody, G.M. 2002: Status of land cover classification accuracy assessment. *Remote Sensing of Environment* 80, 185–201.

Franklin, S.E. and **Wulder, M.A.** 2002: Remote sensing methods in medium spatial resolution satellite data land cover classification of large areas. *Progress in Physical Geography* 26, 173–205.

Franklin, S.E., He, Y., Pape, A.D., Guo, X. and **McDermid, G.J.** 2009: A quantitative comparison of SPOT and ASTER imagery for replacing Landsat in large-area mapping programs. *International Journal of Remote Sensing*, in press.

Gamba, P. and **Chanussot, J.** 2008: Guest editorial: Foreword to the special issue on data fusion. *IEEE Transactions on Geoscience and Remote Sensing* 46, 1283–88.

Gao, F., Masek, J., Schwaller, M. and **Hall, F.** 2006: On the blending of the Landsat and MODIS surface reflectance: predicting daily Landsat surface reflectance. *IEEE Transactions on Geoscience and Remote Sensing* 44, 2207–18.

Garcia-Gigorro, S. and **Saura, S.** 2005: Forest fragmentation estimated from remotely sensed data: is comparison across scales possible? *Forest Science* 5, 51–63.

Garzelli, A. 2002: Wavelet-based fusion of optical and SAR image data over urban area. Retrieved 18 September 2009 from http://www.isprs.org/commission3/proceedings02/papers/paper054.pdf

Gelautz, M., Paillou, P., Chen, C.W. and **Zebker H.A.** 2003: Radar stereo- and interferometry-derived digital elevation models: comparison and combination using Radarsat and ERS-2 imagery. *International Journal of Remote Sensing* 20, 5243–64.

Griffin, M.K., Hsiao-hua, K.B., Mandl, D. and **Miller, J.** 2003: Cloud cover detection algorithm for EO-1 Hyperion imagery. *Proceedings of SPIE* 5093, 483.

Gutman, G.G. 1992: Satellite daytime image classification for global studies of earth's surface parameters from polar orbits. *International Journal of Remote Sensing* 13, 3295–304.

Guyenne, T.D. 1995: ERS-1/2 multitemporal tandem image: Helsinki (Finland). *Supplement to Earth Observation Quarterly* 48, 4.

Hall, L.S., Krausman, P.R. and **Morrison, M.L.** 1997: The habitat concept and a plea for standard terminology. *Wildlife Society Bulletin* 25, 173–82.

Hansen, M.J., Franklin, S.E., Woudsma, C.G., and **Peterson, M.** 2001: Caribou habitat mapping and fragmentation analysis using Landsat MSS, TM, and GIS data in the North Columbia Mountains, British Columbia, Canada. *Remote Sensing of Environment* 77, 50–65.

Hegarat-Mascle, S.L., Bloch, I. and **Vidal-Madjar, D.** 1998: Introduction of neighborhood information in evidence theory and application to data fusion of radar and optical images with partial cloud cover. *Pattern Recognition* 31, 1811–23.

Huang, C., Geiger, E.L. and **Kupfer, J.A.** 2006: Sensitivity of landscape metrics to classification scheme. *International Journal of Remote Sensing* 27, 2927–48.

Hyde, P. 2005: Measuring and mapping forest wildlife habitat characteristics using LIDAR remote sensing and multi-sensor fusion. PhD thesis, University of Maryland.

Jensen, J.R. 2007: *Remote sensing of the environment: an Earth resource perspective* (second edition). Upper Saddle River, NJ: Pearson Prentice Hall.

Jin, Y. and **Wang, D.** 2009: Automatic detection of terrain surface changes after Wenchuan earthquake, May 2008, from ALOS SAR images using 2EM-MRF method. *IEEE Geoscience and Remote Sensing Letters* 6, 344–48.

Justice, C., Belward, A., Morisette, J., Lewis, P., Privette, J. and **Baret, F.** 2000: Developments in the 'validation' of satellite sensor products for the study of the land surface. *International Journal of Remote Sensing* 21, 3383–90.

Kansas, J.L. 2002: Status of the grizzly bear (*Ursus arctos*) in Alberta. Alberta Wildlife Status Report 37. Edmonton: Alberta Conservation Association and Alberta Sustainable Resource Development.

Kent, M. 2007: Biogeography and landscape ecology. *Progress in Physical Geography* 31, 345–55.

Keys, L.D., Schmidt, N.J. and **Phillips, B.E.** 1990: A prototype example of sensor fusion used for a siting analysis. *Technical Papers 1990, ACSM-ASPRS Annual Conference Image Processing and Remote Sensing* 4, 238–49.

Lam, N.S.N. and **Quattrochi, D.A.** 1992: On the issues of scale, resolution, and fractal analysis in the mapping sciences. *Professional Geographer* 44, 88–98.

Leprince, S., Barbot, S., Ayoub, F. and **Avouac, J.** 2007: Automatic and precise orthorectification, coregistration, and subpixel correlation of satellite images, application to ground deformation measurements. *IEEE Transactions on Geoscience and Remote Sensing* 45, 1529–58.

Li, H. and **Wu, J.** 2004: Use and misuse of landscape indices. *Landscape Ecology* 19, 389–99.

Li, Q., Hu, B. and **Pattey, E.** 2008: A scale-wise model inversion method to retrieve canopy biophysical parameters from hyperspectral remote sensing data. *Canadian Journal of Remote Sensing* 34, 311–19.

Lu, D. and **Weng, Q.** 2007: A survey of image classification methods and techniques for improving classification performance. *International Journal of Remote Sensing* 28, 823–70.

Lubis, A.M. and **Isezaki, N.** 2009: Shoreline changes and vertical displacement of the 2 April 2007 Solomon Islands earthquake Mw 8.1 revealed by ALOS PALSAR images. *Physics and Chemistry of the Earth* 34, 409–15.

McDermid, G.J. 2005: Remote sensing for large-area, multi-jurisdictional habitat mapping. PhD thesis, University of Waterloo.

McDermid, G., McLane, A., Collingwood, A., Hird, J., Faraguna, A., Laskin, D., Linke, J., Cranston, J., Guo, X. and **Franklin, S.** 2008: Remote sensing mapping and research update. In Stenhouse, G. and Graham, K., editors, *Foothills Research Institute Grizzly Bear Program 2007 Annual Report*, Hinton, Alberta, 204 pp.

Meng, Q., Borders, B.E., Cleszewski, C.J. and **Madden, M.** 2009: Closest spectral fit for removing clouds and cloud shadows. *Photogrammetric Engineering and Remote Sensing* 75, 569–76.

Mitchell, S.C. 2005: How useful is the concept of habitat? A critique. *Oikos* 110, 634–38.

Moody, A. and **Woodcock, C.E.** 1995: The influence of scale and the spatial characteristics of landscapes on land-cover mapping using remote sensing. *Landscape Ecology* 10, 363–79.

Morena, L.C., James, K.V. and **Beck, J.** 2004: An introduction to the RADARSAT-2 mission. *Canadian Journal of Remote Sensing* 30, 221–34.

Morrison, M.L., Marot, B.G. and **Mannan, R.W.** 2006: *Wildlife-habitat relationships: concepts and application* (third edition). Washington, DC: Island Press, 128 pp.

O'Neill, R.V., Krummel, J.R., Gardner, R.H., Sugihara, G., Jackson, B., DeAngelis, D.L., Milne, B.T., Turner, M.G., Zygnut, B., Christensen, S.W., Dale, V.H. and **Graham, R.L.** 1988: Indices of landscape pattern. *Landscape Ecology* 1, 152–62.

Osborne, P.E., Alonso, J.C. and **Bryant, R.G**. 2001: Modelling landscape-scale habitat use using GIS and remote sensing: a case study with great bustards. *Journal of Applied Ecology* 38, 458–71.

Paillou, P., Schuster, M., Tooth, S., Farr, T., Rosenqvist, A., Lopez, S. and **Malezieux, J.-M.** 2009: Mapping of a major paleodrainage system in eastern Libya using orbital imaging radar: the Kufrah River. *Earth and Planetary Science Letters* 277, 327–33.

Pape, A.D. and **Franklin, S.E.** 2008: MODIS-based change detection for Grizzly Bear habitat mapping in Alberta. *Photogrammetric Engineering and Remote Sensing* 74, 973–85.

Pohl, C. and **van Genderen, J.L.** 1995: Image fusion of microwave and optical remote sensing data for map updating in the tropics. *Image and Signal Processing for Remote Sensing, Proceedings EUROPTO 95, SPIE* 2579, 2–10.

— 1998: Multisensor image fusion in remote sensing: concepts, methods and applications. *International Journal of Remote Sensing* 19, 823–54.

— 1999: Multi-sensor image maps from SPOT, ERS and JERS. *Geocarto International* 14, 34–41.

Powell, R.L., Matzke, N., de Souza, C. Jr, Clark, M., Numata, I., Hess, L.L. and **Roberts, D.A.** 2004: Sources of error in accuracy assessment of thematic land-cover maps in the Brazilian Amazon. *Remote Sensing of Environment* 90, 221–34.

Qi, J., Kerr, Y.H., Moran, M.S., Weltz, M., Huete, A.R., Sorooshian, S. and **Bryant, R**. 2000: Leaf area index estimates using remotely sensed data and BRDF models in a semiarid region. *Remote Sensing of Environment* 73, 18–30.

Radarsat-2 Information 2009a: Applications. Retrieved 18 September 2009 from http://www.radarsat2.info/application/index.asp

— 2009b: Features and benefits. Retrieved 18 September 2009 from http://www.radarsat2.info/about/features_benefits.asp

Ranchin, T. and **Wald, L.** 2000: Fusion of high spatial and spectral resolution images: the ARSIS concept and its implementation. *Photogrammetric Engineering and Remote Sensing* 45, 49–61.

Ranson, K.J., Kovacs, K., Sun, G. and **Kharuk, V.I.** 2003: Disturbance recognition in the boreal forest using radar and Landsat-7. *Canadian Journal of Remote Sensing* 29, 271–85.

Rignot, E. 2008: Changes in West Antarctic ice stream dynamics observed with ALOS PALSAR data. *Geophysical Research Letters* 35, L12505, DOI: 10.1029/2008GL033365.

Rogers, R.H. and **Wood, L.** 1990: The history and status of merging multiple sensor data: an overview. *Technical Papers 1990, ACSM-ASPRS Annual Convention, Image Processing and Remote Sensing* 4, 352–60.

Rosenqvist, A., Shimada, M., Ito, N. and **Watanabe, M.** 2007: ALOS PALSAR: a pathfinder mission for global-scale monitoring of the environment. *IEEE Transactions on Geoscience and Remote Sensing* 45, 3307–16.

Rosenqvist, A., Shimada, M., Watanabe, M., Tadono, T. and **Yamauchi, K**. 2004: Implementation of systematic data observation strategies for ALOS PALSAR, PRISM and AVNIR-2. *IEEE Transactions on Geoscience and Remote Sensing* 7, 4527–30.

Rossi, R.E., Dungan, J.L. and **Beck, L.R.** 1994: Kriging in the shadows: geostatistical interpolation for remote sensing. *Remote Sensing of Environment* 49, 32–40.

Roy, D.P., Ju, J., Lewis, P., Schaaf, C., Gao, F., Hansen, M. and **Lindquist, E.** 2008: Multi-temporal MODIS-Landsat data fusion for relative radiometric normalization, gap filling, and prediction of Landsat data. *Remote Sensing of Environment* 112, 3112–30.

Saura, S. 2004: Effects of remote sensor spatial resolution and data aggregation on selected fragmentation indices. *Landscape Ecology* 19, 197–209.

Shao, G. and **Wu, J.** 2008: On the accuracy of landscape pattern analysis using remote sensing data. *Landscape Ecology* 23, 505–11.

Simpson, J.J. and **Stitt, J.R.** 1998: A procedure for the detection and removal of cloud shadow from AVHRR data over land. *IEEE Transactions on Geoscience and Remote Sensing* 36, 880–97.

Stenhouse, G. 2008: Introduction. In Stenhouse, G. and Graham, K., editors, *Foothills Research Institute Grizzly Bear Program 2007 Annual Report*, Hinton, Alberta, 1.

Takada, M., Mishima, Y. and **Natsume, S.** 2009: Estimation of surface soil properties in peatland using ALOS/PALSAR. *Landscape and Ecological Engineering* 5, 45–58.

Thanh, H.N., Ryutaro, T. and **Dinh, D.N.** 2008: Cloud removal of optical image using SAR data for ALOS applications – experimenting on simulated ALOS data. *Proceedings of the Conference of the Remote Sensing Society of Japan* 41, 73–74.

Tseng, D.C., Tseng, H.T. and **Chien, C.L.** 2008: Automatic cloud removal from multi-temporal SPOT images. *Applied Mathematics and Computation* 205, 584–600.

Urban, D.L. 2005: Modeling ecological processes across scales. *Ecology* 86, 1996–2006.

Wang, B., Ono, A., Muramatsu, K. and **Fujiwara, N.** 1999: Automated detection and removal of clouds and their shadows from Landsat TM images. *IEICE Transactions on Information and Systems* E82-D, 453–60.

Wang, Z., Jin, J., Liang, J., Yan, K. and **Peng, Q.** 2005: A new cloud removal algorithm for multi-spectral images. *Proceedings of SPIE, SAR and Multispectral Image Processing (MIPPR 2005)* 6043(2), 60430W.1–11.

Waske, B. and **van der Linden, S.** 2008: Classifying multilevel imagery from SAR and optical sensors by decision fusion. *IEEE Transactions on Geoscience and Remote Sensing* 46, 1457–66.

Weydahl, D.J. 1993: Multitemporal analysis of ERS-1 SAR images over land areas. *Proceedings of the 13th Annual IEEE International Geoscience and Remote Sensing Symposium (IGARSS '93), Better Understanding of Earth Environment, Tokyo* 3, 1459–61.

Wiens, J.A. 1989: Spatial scaling in ecology. *Functional Ecology* 3, 385–97.

Wong, A. and **Clausi, D.** 2007: ARRSI: automatic registration of remote sensing images. *IEEE Transactions on Geoscience and Remote Sensing* 45, 1483–93.

Wu, J. 2004: Effects of changing scale on landscape pattern analysis: scaling relations. *Landscape Ecology* 19, 125–38.

Wu, J. and **Hobbs, R.** 2002: Key issues and research priorities in landscape ecology: an idiosyncratic synthesis. *Landscape Ecology* 17, 355–65.

Wu, J., Shen, W., Sun, W. and **Tueller, P.T.** 2002: Empirical patterns of the effects of changing scale on landscape metrics. *Landscape Ecology* 17, 761–82.

Wulder, M.A., White, J.C., Goward, S.N., Masek, J.G., Irons, J.R., Herold, M., Cohen, W.B., Loveland, T.R. and **Woodcock, C.E.** 2008: Landsat continuity: issues and opportunities for land cover monitoring. *Remote Sensing of Environment* 112, 955–69.

Xu, M., Watanachaturaporn, P., Varshney, P.K. and **Arora, M.K.** 2005: Decision tree regression for soft classification of remote sensing data. *Remote Sensing of Environment* 97, 322–36.

Yamanouchi, T. and **Kawaguchi, S.** 1992: Cloud distribution in the Antarctic from AVHRR data and radiation measurements at the surface. *International Journal of Remote Sensing* 13, 111–27.